Supplementary Information

Intensified Gas Diffusion in Ordered Mesoporous PtCo Alloys for Enhanced Oxygen Reduction Electrocatalysis

Kunming Song[a,b,c,#], Fantao Kong[b,#] , Ruxiang Shen[b], Xu Yu[b], Han Tian[b], Qiuyun Guo[a,b,c],Gang Zhang[d] , Wenping Sun[e] and Xiangzhi Cui[a,b,c,e] *

a. School of Chemistry and Materials Science, Hangzhou Institute for Advanced Study, University of Chinese Academy of Sciences, Hangzhou 310024, PR China.

b. State Key Lab of High Performance Ceramics and Superfine Microstructure, Shanghai Institute of Ceramics, Chinese Academy of Sciences, Shanghai 200050, PR China.

c. Center of Materials Science and Optoelectronics Engineering, University of Chinese Academy of Sciences, Beijing 100049, PR China.

d. Shanghai Motor Vehicle Inspection Certification & Tech Innovation Center Co., Ltd.

e. State Key Laboratory of Clean Energy Utilization,Zhejiang University, Hangzhou 310027, P. R. China.

** Email: cuixz@mail.sic.ac.cn (X. Cui).*

 # These authors contributed equally to this work.

Chemicals

Pluronic P123 (PEO_{20}-PPO_{70}-PEO_{20}, Purity 99%) was obtained from Sigma-Aldrich. Potassium platinochloride (K_2PtCl_4, 98%+), Cobalt (II) Iodide (CoI_2,99.5%), L(+)-Ascorbic Acid ($C_6H_8O_6$,99%), $Pt(acac)_2$ and $Co(acac)_2$ were purchased from Adamas. Nafion (5 wt %) were purchased from Dupont. Hydrochloric acid (HCl), ammonia solution ($NH_3 \bullet H_2O$, 50%), 1-butanol tetraethoxysilane (TEOS), Acetone(CH_3COCH_3), perchloric acid ($HClO_4$, 70–72%) and ethanol (CH_3CH_2OH, 99%) were purchased from Sinopharm Chemical Reagent Co. Ltd. (Shanghai, China).

Synthesis of KIT-6-x.

In a typical synthesis, 6 g of P123 was combined with 217 g of distilled water and 11.8 g of concentrated HCl (35%), followed by the addition of 6 g of butanol. After stirring for one hour, 12.9 g of TEOS was added while keeping the temperature at 35 °C. The mixture was then stirred for an additional 24 hours at this temperature. Subsequently, a hydrothermal treatment was conducted, heating the mixture for 24 hours at either 70, 100, or 130 °C in a sealed polypropylene container. The resultant solid was filtered and dried at 80 °C. Finally, KIT-6-'x' was produced after being washed with an ethanol/HCl solution and calcined in air at 550 °C, where 'x' indicates the average pore diameter of KIT-6.

Synthesis of Pt/KIT-6.

In a typical synthesis, a mixture of 0.30 g of KIT-6 and 80.0 mg of K2PtCl4 were mixed in 2.0 mL of water, which was then dried under vacuum to form a powder. Subsequently, 2.0 mL of a freshly prepared solution of L-ascorbic acid (AA) at 0.25 M was added dropwise to the powder to initiate the crystallization of meso-Pt within the mesoporous KIT-6. The reaction was conducted at room temperature for 10 hours, and afterward, the product was washed and dried to obtain Pt/KIT-6.

Synthesis of PtCo-meso.

In a typical synthesis of PtCo-meso, 200 mg of the product from the previous step (Pt/KIT-6) was mixed and ground with 138 mg of CoI_2 for 10 minutes to ensure uniform

mixing. Anneal the mixture at 500 °C in a hydrogen argon atmosphere for 15 hours to obtain the product (PtCo/KIT-6). The template was etched and removed using 10% HF, centrifuged, washed and freeze dried to obtain the product: PtCo-meso$_{4.5}$. The preparation of PtCo-meso with different pore sizes was carried out using KIT-6, while other conditions remained unchanged.

Synthesis of PtCo/C

Typically, for preparing PtCo/C catalysts, 150 mg of Pt(acac)$_2$ and 150 mg of Co(acac)$_2$ were dissolved in 20 ml acetone, and followed by sonicating for 10 min to form a homogeneous solution. Then, 200 mg of carbon black was dispersed into above solution under ultrasonic for 30 min.The mixture was dried in air at 80 °C for 2 h with a heating rate of 2 °C/min. Subsequently, the dried mixture was reduced at 700 °C in a 5 vol% H_2/Ar with a heating rate of 5 °C/min. When cooling to room temperature, the powder was carefully transferred from the tube furnace. The final PtCo/C alloy catalyst was obtained by etching the partial Co in a 1.0 mol/L H_2SO_4 solution.

Material characterizations

The samples' nitrogen adsorption-desorption isotherms, specific surface area, and pore size distribution were assessed via the Brunauer-Emmett-Teller (BET) method using a Micromeritics ASAP 2460 system (USA). Imaging through scanning electron microscopy (SEM) was carried out with a FEI Magellan-400 field emission scanning electron microscope at 5 kV. For transmission electron microscopy (TEM), which included high-resolution transmission electron microscopy (HRTEM), high-angle annular dark field scanning TEM (HAADF-STEM), energy dispersive X-ray spectrometry (EDS), and corresponding EDS mapping, a FEI Tecnai G2 F20 field emission transmission electron microscope was utilized. Powder X-ray diffraction (XRD) patterns were obtained at a scan rate of 4° min^{-1} with a Rigaku D/Max-2550 V X-ray diffractometer featuring a Cu Kα radiation source (40 kV, 40 mA). Data from X-ray photoelectron spectroscopy (XPS) were collected using a Thermo Fisher Scientific ECSAlab250 XPS spectrometer with monochromatic Al Kα radiation. Before characterization, the catalysts underwent Ar ion etching. In situ Raman spectroscopy

was performed concurrently with cyclic voltammetry scans in a specialized three-electrode spectroscopic electrochemical Raman cell (Xplora Plus).

Electrochemical testing

At room temperature, ORR electrochemical measurements were carried out using a three-electrode arrangement that included a RRDE linked to a CHI 660E electrochemical workstation from Shanghai Chenhua Instrument Corporation, China. The counter electrode was a carbon rod, while an Ag/AgCl electrode served as the reference. All potentials were referenced to a reversible hydrogen electrode (RHE) for the purpose of conversion.

For the preparation of the nanocatalyst ink, 1.0 mg of PtCo-meso and 2.0 mg of Vulcan XC-72 carbon were mixed with 800 µl of ethanol. The mixture was sonicated for 30 minutes, after which 30 µl of a 5% Nafion solution was incorporated. It was then sonicated for an additional 10 minutes to achieve a uniform catalyst ink solution.For the commercial Pt/C catalyst, 3 mg of the catalyst was mixed with 800 µl of isopropanol and 30 µl of a 5% Nafion solution, and then sonicated for 1 hour. Subsequently, 10 µl of the resulting ink was applied to the Rotating Ring-Disk electrode (RRDE), which has a geometric area of 0.2475 cm^2.

In a 0.1 M $HClO_4$ electrolyte saturated with nitrogen, cyclic voltammograms (CVs) were measured at a sweep rate of 50 mV s^{-1}. The electrochemical active surface area (ECSA) of Pt-based catalysts in acidic electrolytes can be determined from CV curves by analyzing the area related to the hydrogen adsorption and desorption peaks. This area corresponds to Q_H, which represents the hydrogen adsorption.

$$ECSA = \frac{{Q_H}/{V}}{0.21\left(mC \cdot cm^{-2}\right) \cdot M_{Pt}}$$

Q_H is the hydrogen adsorption area calculated from the CV curve in mC cm^{-2}. V is the sweep speed in V s^{-1}. M_{Pt} is the catalyst mass on the electrode surface in mg cm^{-2}.

The polarization curves for the ORR were obtained by sweeping the potential from 0.05 to 1.05 V_{RHE} in a 0.1 M $HClO_4$ solution saturated with oxygen, at a rotation speed

of 1600 rpm and a sweep rate of 10 mV s^{-1}. The accelerated stability tests (ASTs) were performed by conducting cyclic sweeps within a range of 0.6 to 1.0 V_{RHE} in an O_2-saturated 0.1 M $HClO_4$ electrolyte, using a sweep rate of 100 mV s^{-1} while altering the number of cycles.

The gas diffusion electrode (GDE) technique was utilized to assess the electrocatalytic performance and oxygen transport efficiency of catalyst layers within a three-electrode electrochemical testing setup. This setup included a carbon paper electrode coated with a catalyst film (0.502 cm^2, serving as the working electrode), a platinum filament as the counter electrode, and an Ag/AgCl reference electrode. The catalyst ink was applied to the carbon paper to create a uniform working electrode, with platinum loading maintained at 0.04 mg cm^2. Electrochemical assessments were carried out in a 4.0 M HClO4 solution for the oxygen reduction reaction (ORR). Linear sweep voltammetry (LSV) curves were obtained in O_2-saturated 4.0 M $HClO_4$ at a scan rate of 50 mV s^{-1}. The accelerated stress test (AST) was performed in O_2-saturated 4.0 M $HClO_4$ by executing cyclic potential sweeps between 0.05 and 1.1 V vs. RHE at a rate of 100 mV s^{-1} over 100 cycles.

MEA fabrication and test

The catalytic performance was assessed under the operational conditions of a proton exchange membrane fuel cell (PEMFC). Initially, 12 mg of catalyst was dissolved in 2 ml of isopropanol. A specific amount of Nafion® (5%) ionomer was then added to create a solution with a defined ionomer/carbon ratio (I/C ratio). This ink was subsequently sprayed onto the Proton Exchange Membrane (Gore MX765.08). A catalyst-coated membrane (CCM) with an active geometric area of 4 cm^2 was placed onto a gas diffusion layer (Toray TGP-H060). Cathode catalysts included PtCo-$meso_{2.4}$/C, PtCo-$meso_{4.8}$/C, PtCo-$meso_{7.1}$/C, and a commercial Pt/C (20 wt% loading, Hesen), with Pt loading at the cathode set at 0.20 mg_{Pt} cm^{-2} for both PtCo-meso and commercial Pt/C. For the anode, a commercial Pt/C catalyst (40 wt% loading, Hesen) was utilized at a loading of 0.1 mg_{Pt} cm^{-2}. Fuel cell testing was conducted using a Scribner 850e system, with the membrane electrode assembly (MEA) sandwiched

between graphite plates featuring single serpentine flow channels. Pressure differentials at the cathode and anode were monitored using sensors connected to the cell's inlet and outlet while operating at 80°C, 200 kPa (absolute) back pressure, 100% relative humidity (RH), a hydrogen flow rate of 500 mL min^{-1}, and an oxygen/air flow rate of 700 mL min^{-1}. Polarization curves were obtained via potential step mode at 50 mV increments, holding each point for 2 minutes. Accelerated stability tests (ASTs) were conducted at 80 °C, 200 kPa (abs), and 100% RH with hydrogen/nitrogen for the anode/cathode, including 30,000 cycles of cyclic voltammetry (CV) with potential ranging from 0.6 V to 0.95 V.

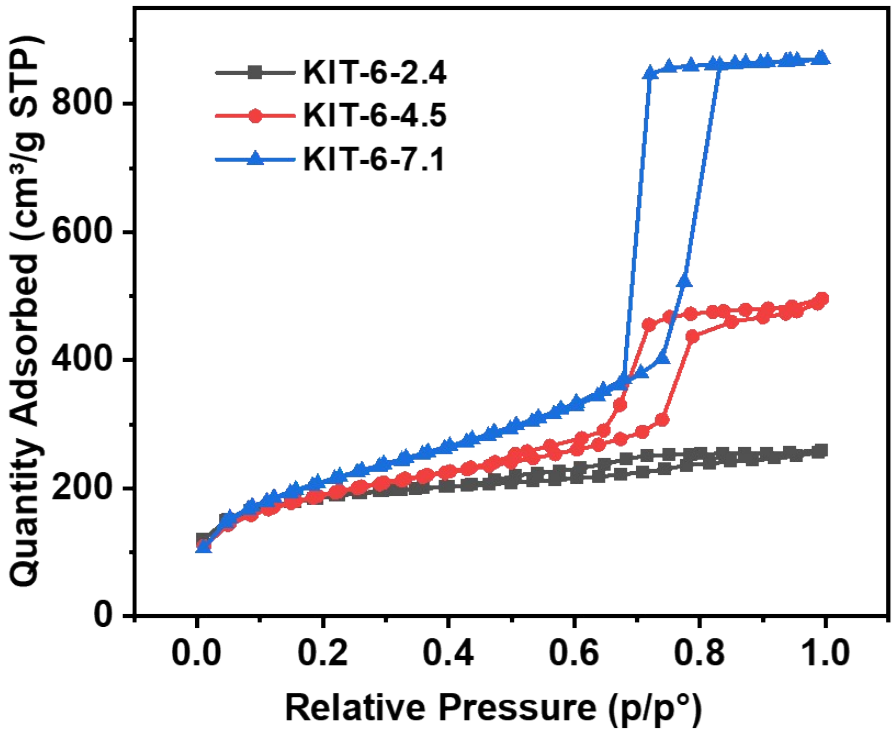

Figure S1. N_2 sorption isotherms of PtCo-meso$_x$.

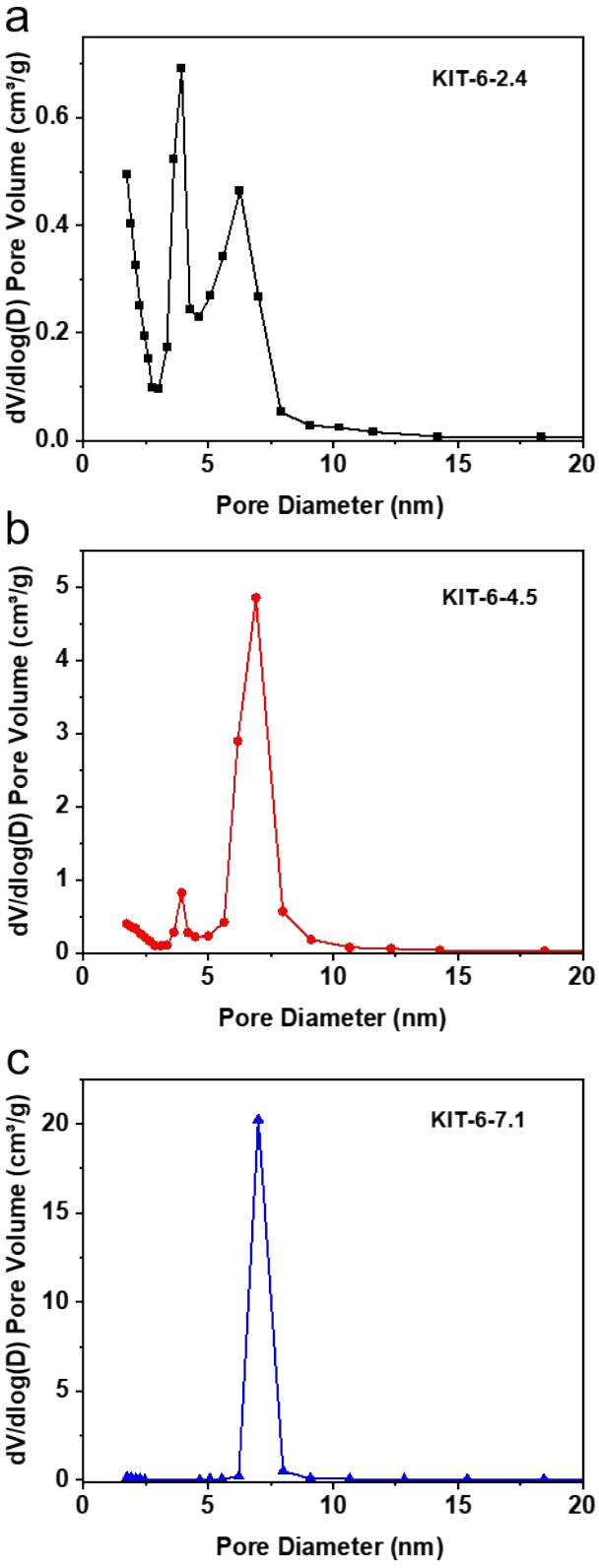

Figure S2. Pore size distributions of KIT-6-x samples.

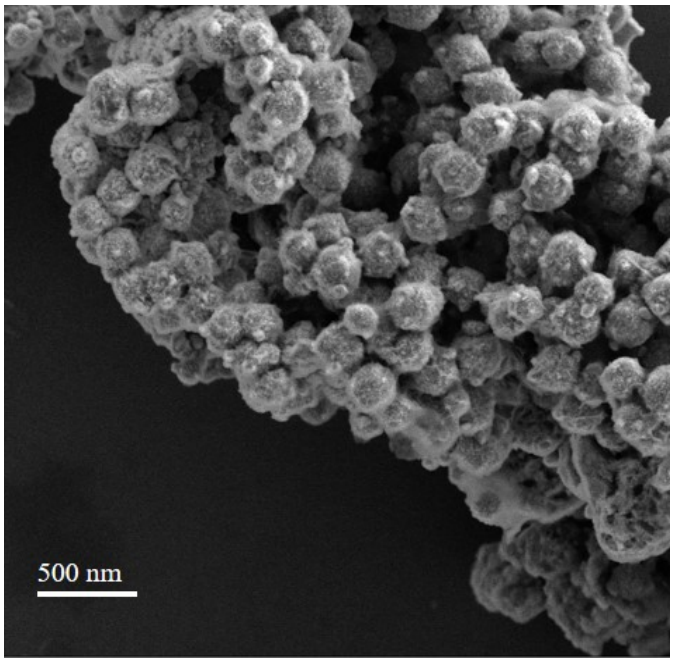

Figure S3. SEM image of PtCo-meso$_{4.5}$.

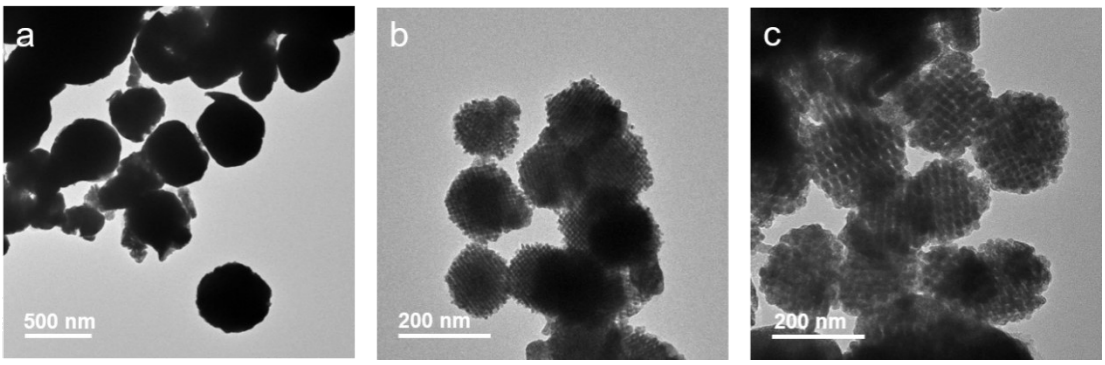

Figure S4. TEM images of PtCo-meso$_X$. (a) PtCo-meso$_{2.4}$, (b) PtCo-meso$_{4.5}$ and (c) PtCo-meso$_{7.1}$.

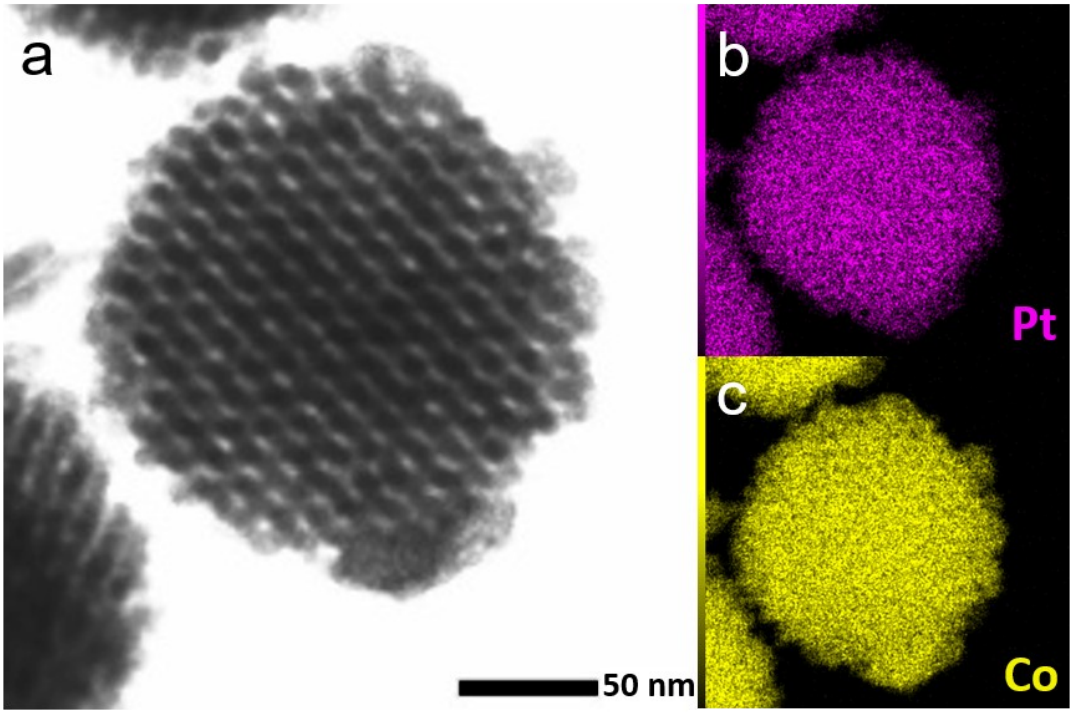

Figure S5. (a) HADDF-STEM image, and (b, c) EDS element mapping of PtCo-meso$_{2.4}$.

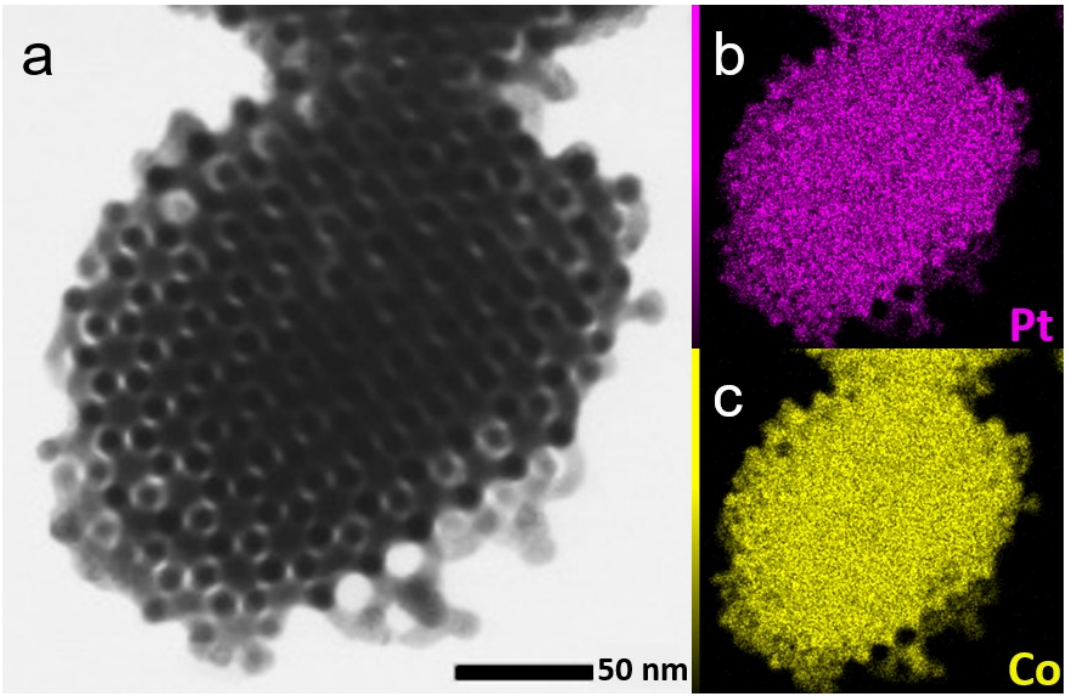

Figure S6. (a) HADDF-STEM image and (b, c) EDS element mapping of PtCo-meso$_{7.1}$.

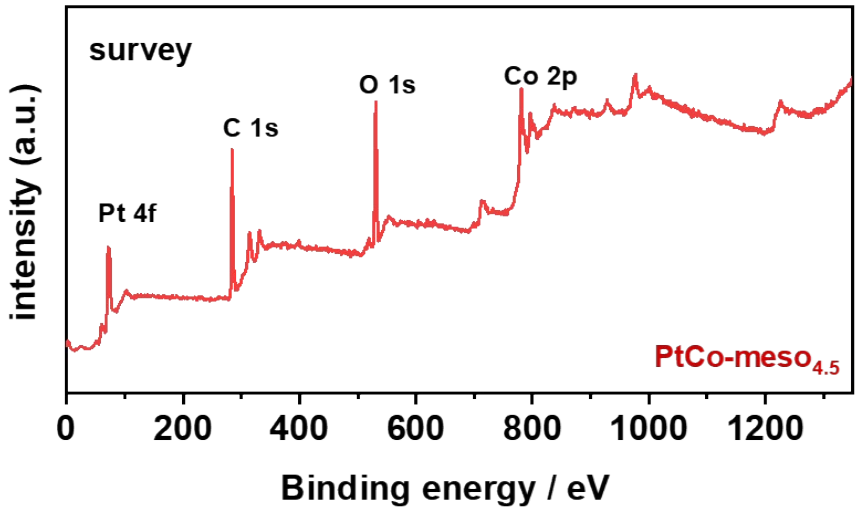

Figure S7. XPS survey spectrum of PtCo-meso$_{4.5}$.

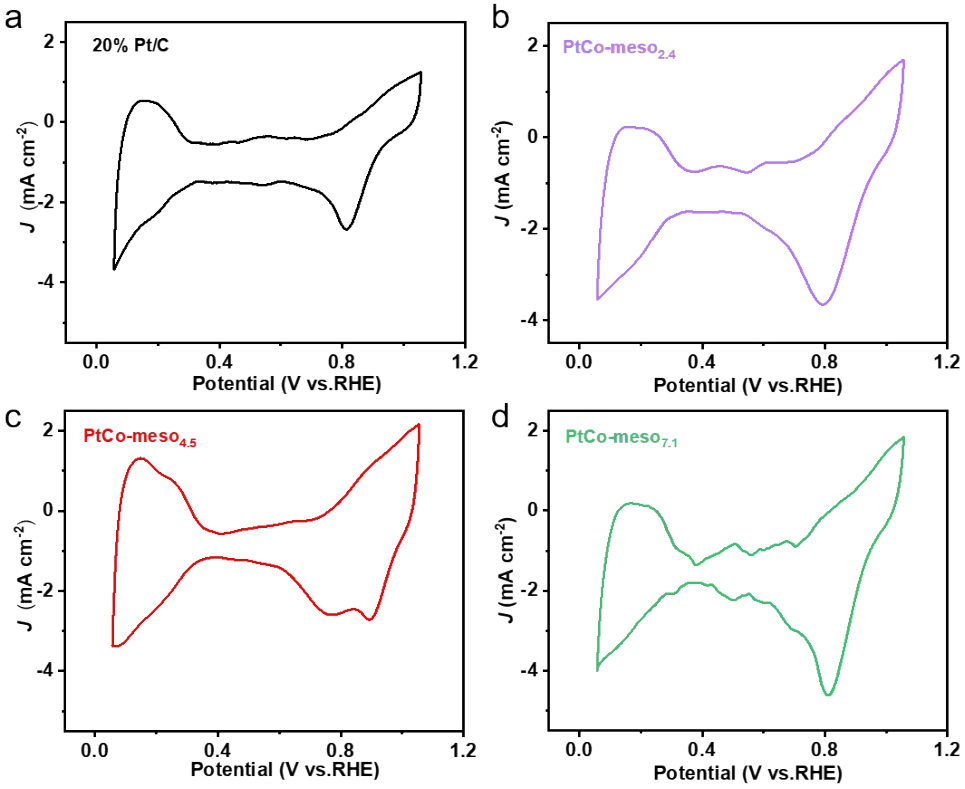

Figure S8. CV curves of (a) Pt/C and (b-d) PtCo-meso$_x$.

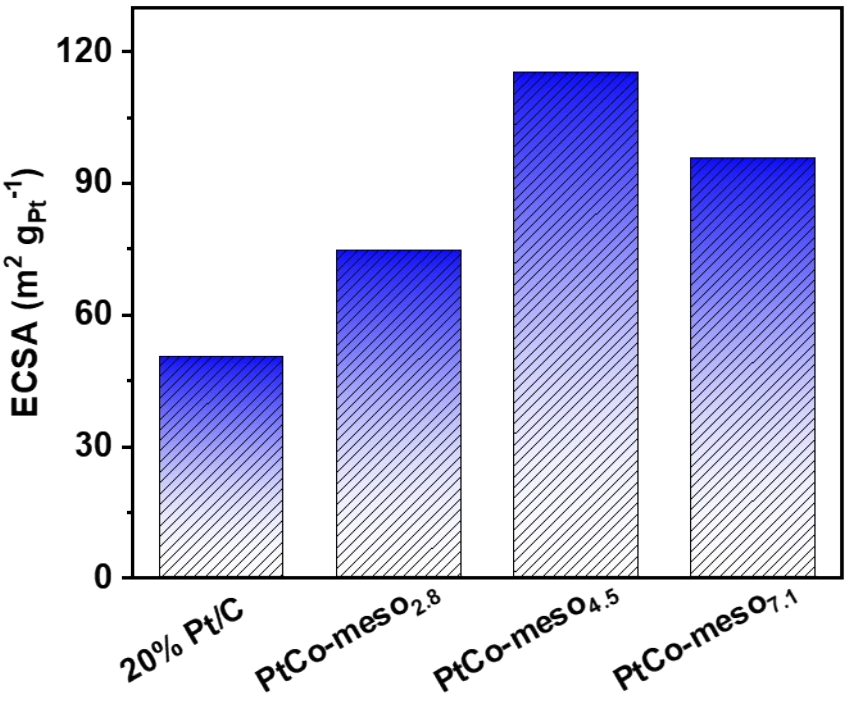

Figure S9. Histograms of ECSA of Pt/C and PtCo-meso$_x$.

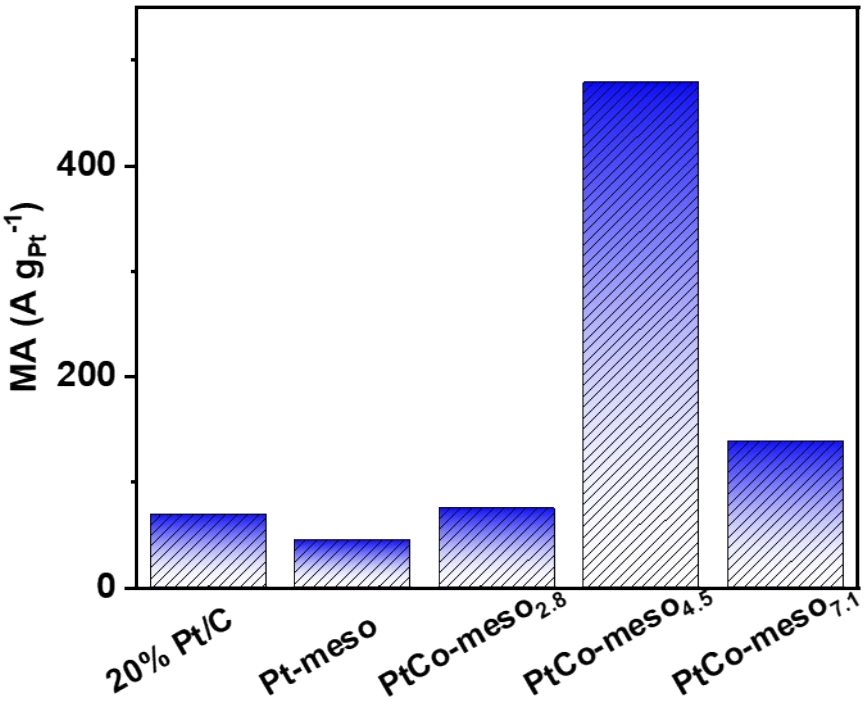

Figure S10. Histograms of MA of Pt/C and PtCo-meso$_x$.

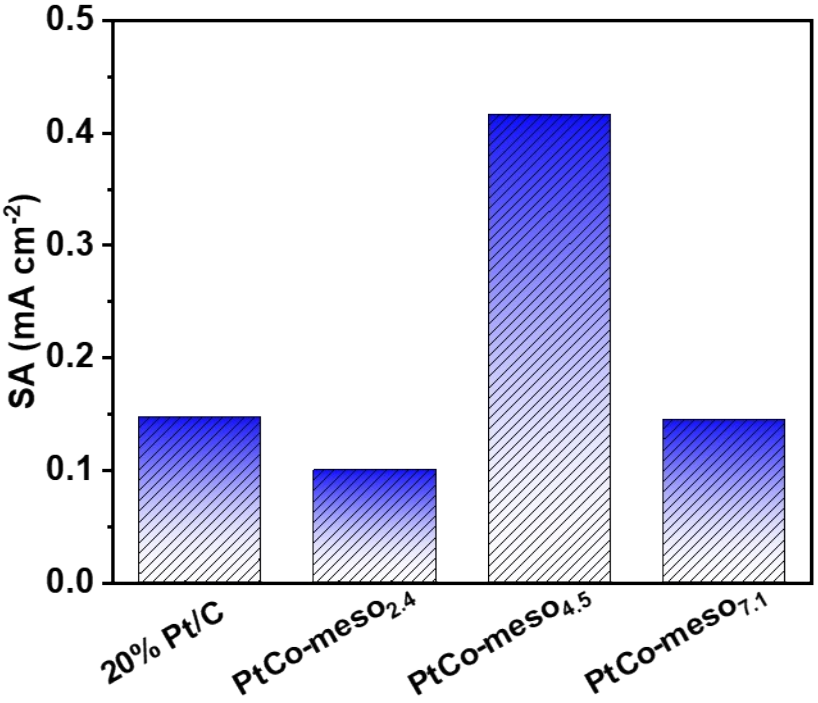

Figure S11. Histograms of SA of Pt/C and PtCo-meso$_x$.

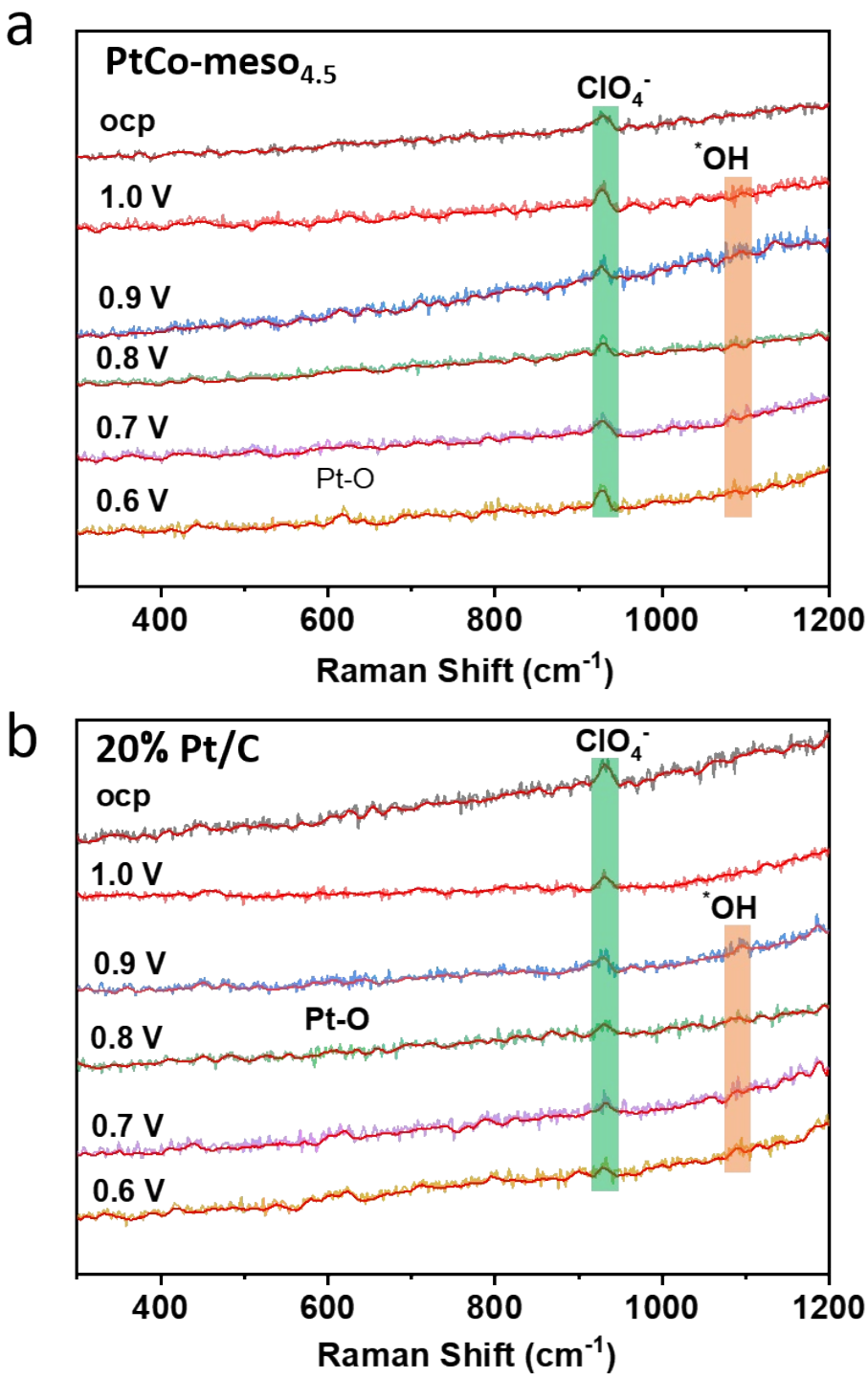

Figure S12. In-situ Raman spectra of (a) PtCo-meso$_{4.5}$ and (b) Pt/C.

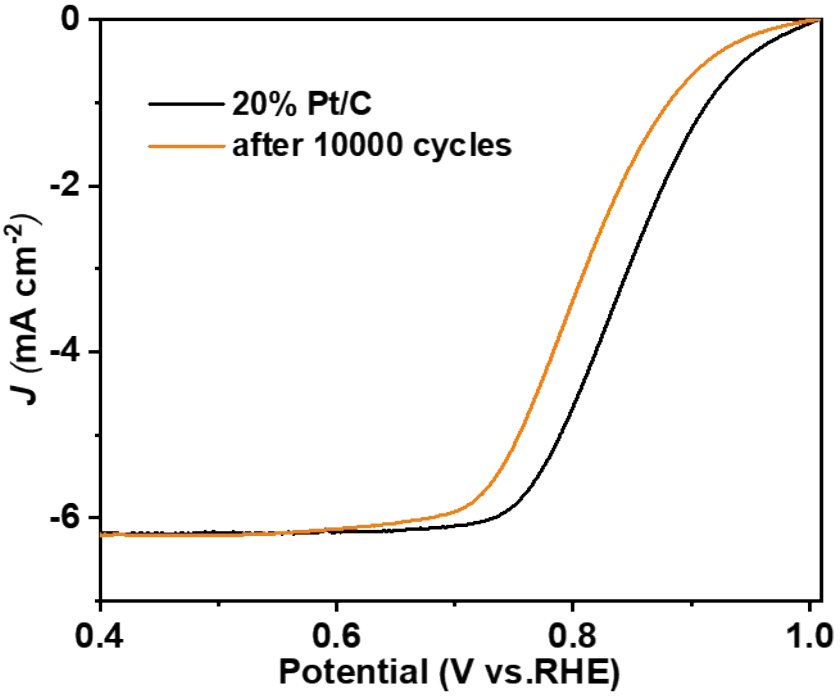

Figure S13. LSV curves of Pt/C before and after ADTs of Pt/C.

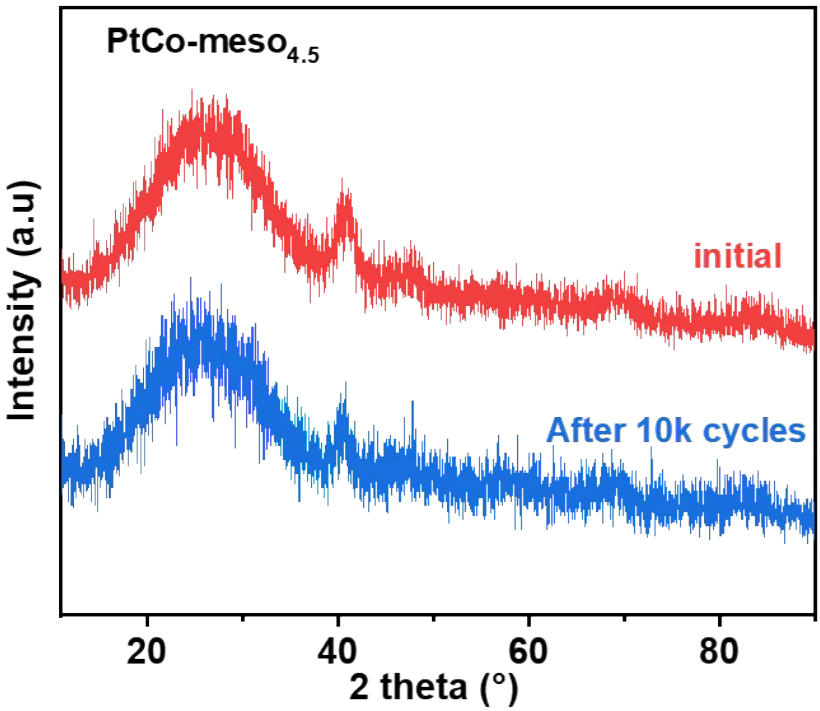

Figure S14. XRD spectra of PtCo-meso$_{4.5}$ before and after 10k AST cycles.

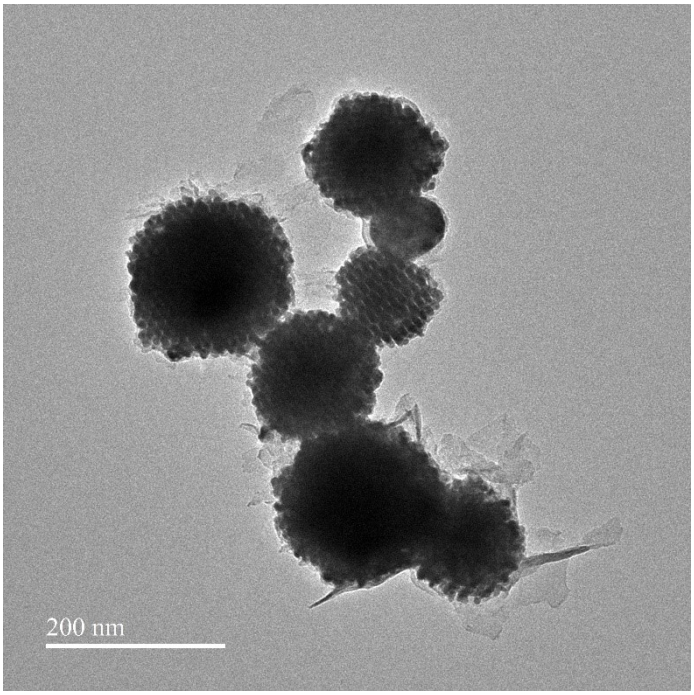

Figure S15. TEM image of PtCo-meso$_{4.5}$ after 10k AST cycles.

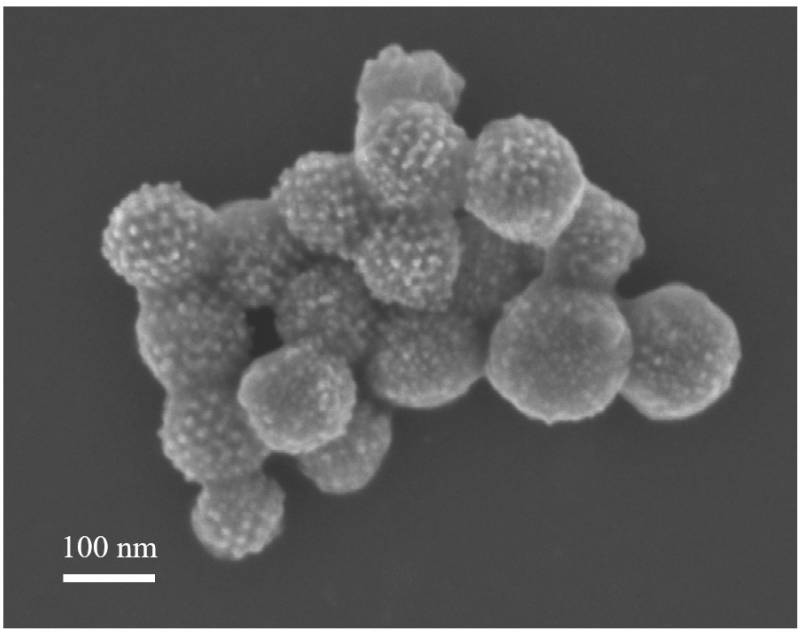

Figure S16. SEM image of PtCo-meso$_{4.5}$ after 10k AST cycles.

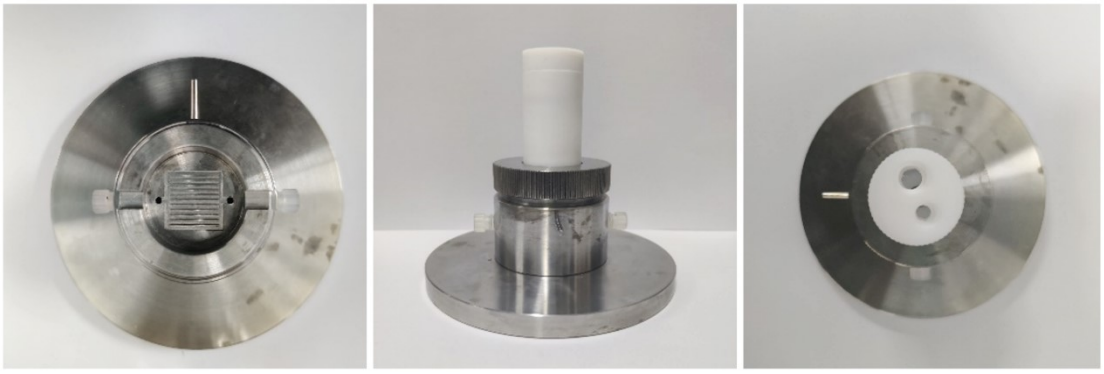

Figure S17. Photograph of the gas diffusion electrode.

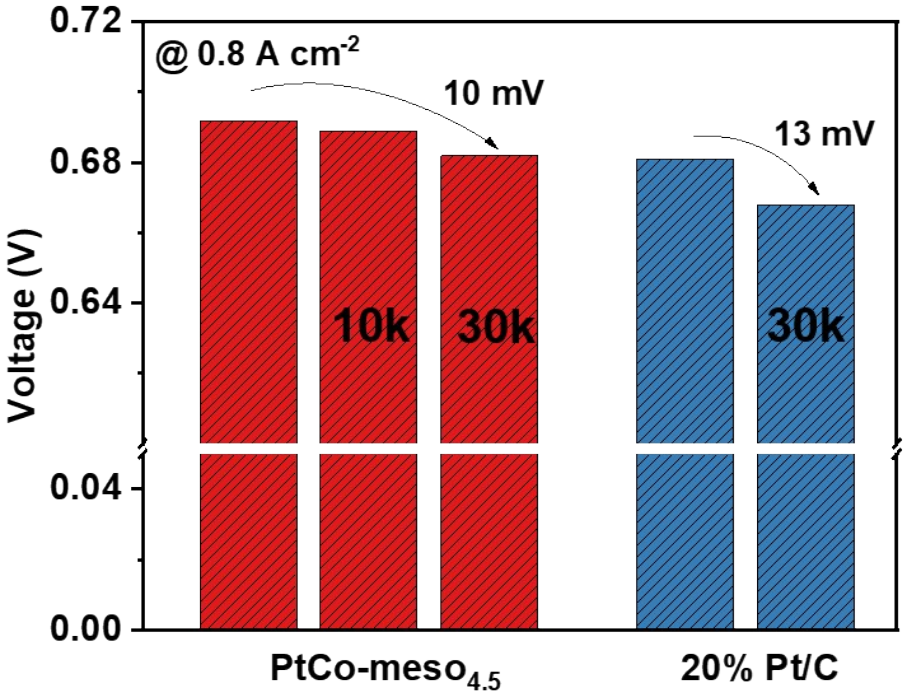

Figure S18. Histograms of the initial potential of PtCo-meso$_{4.5}$ and Pt/C at 0.8 A cm^{-2} and the potentials after 10K and 30K ADT cycles.

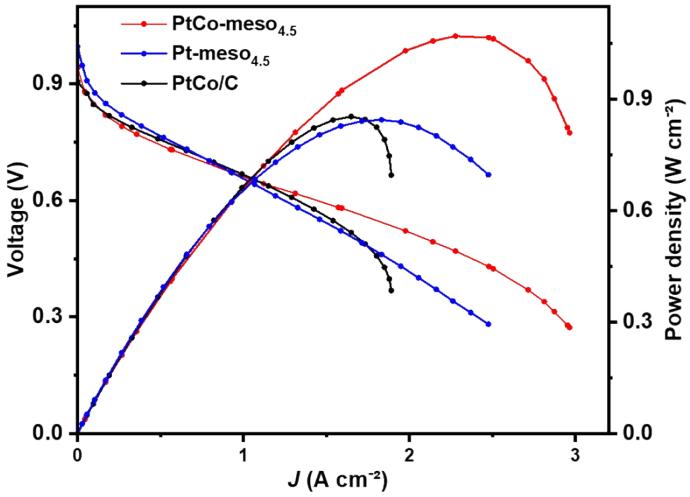

Figure 19. Polarization and power density curves of PtCo-meso$_{4.5}$,Pt-meso$_{4.5}$ and 20% Pt/C as the air cathode assembled in H_2-air fuel cell.

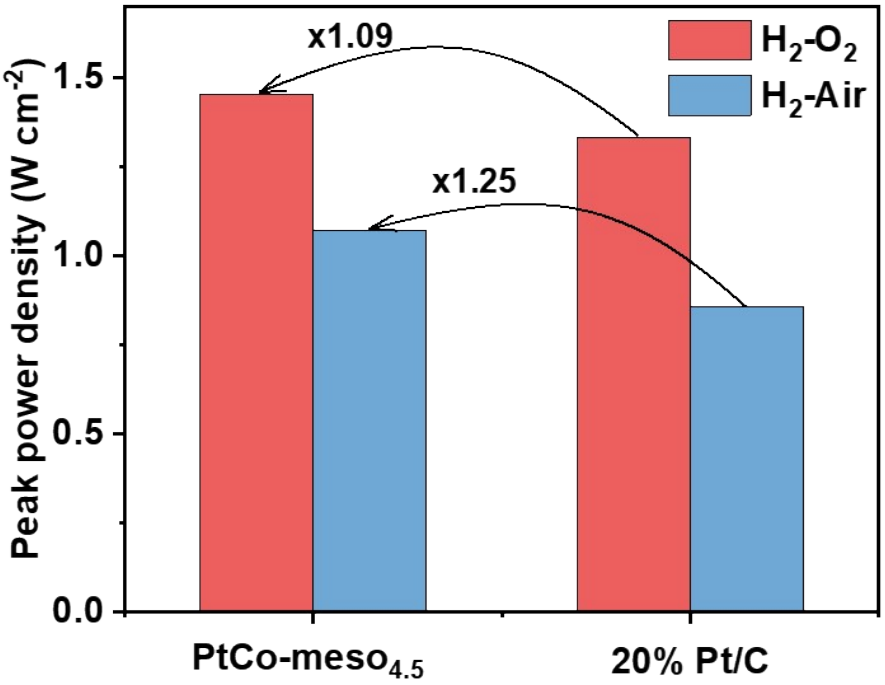

Figure S20. Comparison of peak power density of PtCo-meso$_{4.5}$ and 20% Pt/C under H_2-O_2 and H_2-Air conditions, respectively.

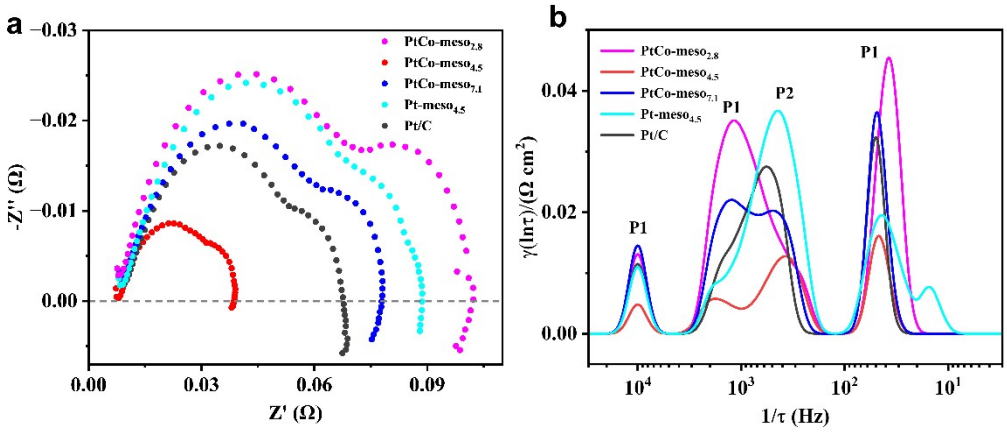

Figure 21. Electrochemical impedance analysis under the standard operating condition;(a) Nyquist plot of PtCo-meso$_x$,Pt-meso$_{4.5}$ and 20% Pt/C; (b) DRT analysis.

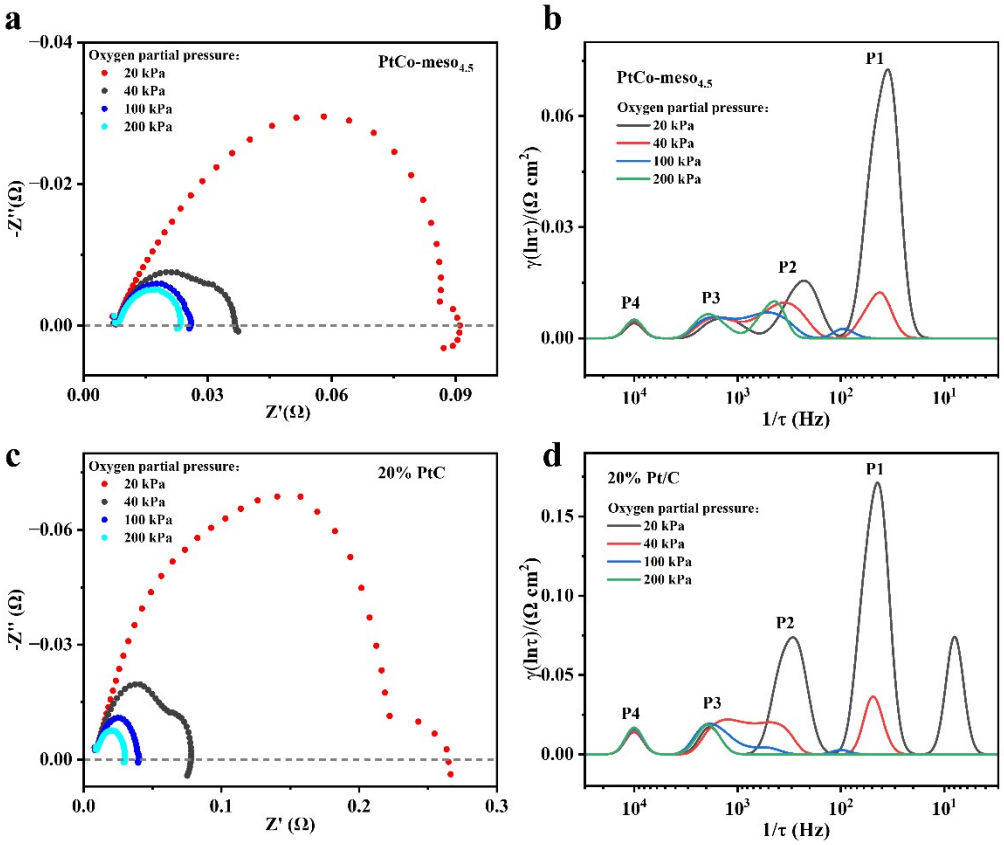

Figure 22. Electrochemical impedance analysis under different oxygen partial pressure operating conditions; (a) Nyquist plot and (b) DRT analysis of PtCo-meso$_{4.5}$; (a) Nyquist plot and (b) DRT analysis of Pt/C.

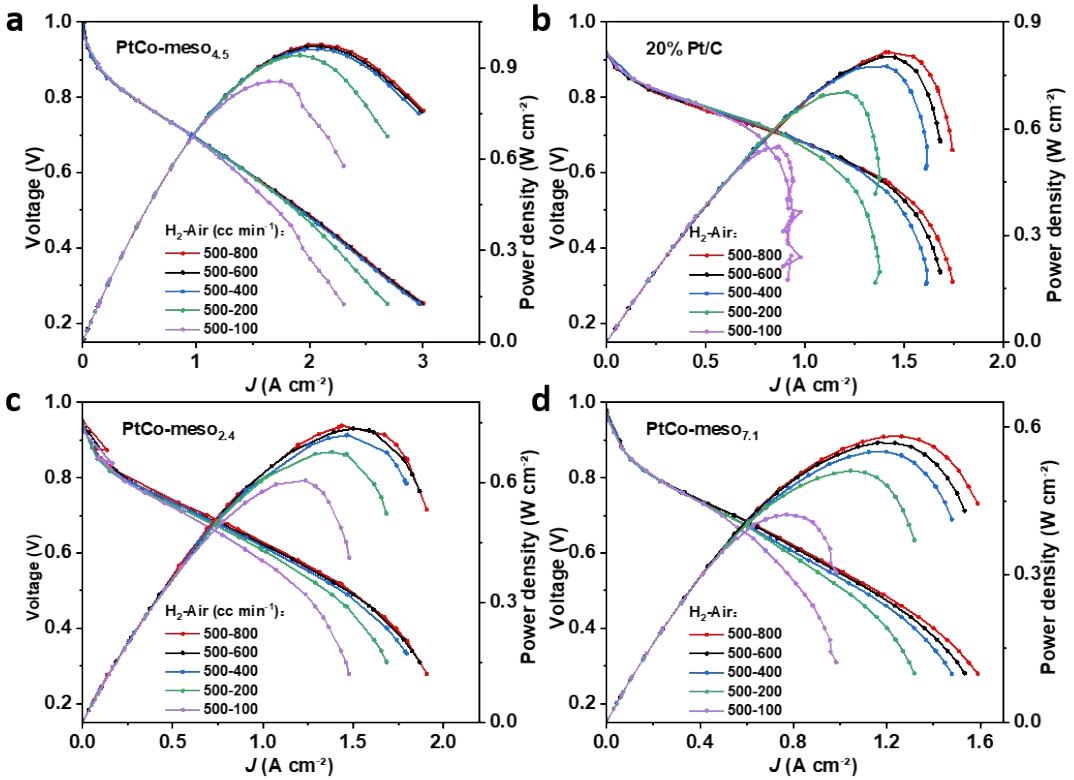

Figure S23. Fuel cell polarization plots and Power density curve with different air flow rates of (a) PtCo-meso$_{4.5}$, (b) Pt/C, (c) PtCo-meso$_{2.4}$, and (d) PtCo-meso$_{7.1}$.

Table S1. The average pore size and specific surface area of KIT-6-x.

Samples	1	2	3
Average pore diameter (nm)	2.37	4.49	7.06
Specific surface area (m^2g^{-1})	676.26	683.78	762.62

Table S2. Performance comparison of recent carbon supported electrocatalysts in hydrogen-air fuel cells. #: No specific figures are given in the representative text, which is estimated from the article pictures

Catalysts	Anode Pt loading (mg cm^{-2})	Cathode Pt loading (mg cm^{-2})	Current density at 0.6 V (A cm^{-2})	Power density (mW cm^{-2})	Back pressure (MPa)	Refer-ences
PtCo-meso$_{4.5}$	0.1	0.2	1.44	1070	0.2	**This work**
PtCo-meso$_{2.4}$	0.1	0.2	0.86	566	0.2	
PtCo-meso$_{7.1}$	0.1	0.2	1.09	734	0.2	
JM Pt/C	0.1	0.2	1.25	858	0.2	
PtNi/C	0.15	0.15	0.64	490#	without	**1**
PtNi-BNSs	0.1	0.15	1.0	700	0.2	**2**
L10-PtZn	0.1	0.104	1.3#	800#	0.15	**3**
D-Pt_3Co/C	0.1	0.1	1.21	765#	0.15	**4**
CoZ-60Pt	0.1	0.2	1.48	932	0.2	**5**
PtFe@C	0.2	0.2	0.56#	630	0.2	**6**
PtCo30Ni10 @ NG	without	without	1.3#	867	0.15	**7**
PtMg/C-31	0.05	0.1	1.05#	700	0.2	**8**
O-L10-PtCo/C	0.1	0.1	1.34	807	0.2	**9**
T-L10-PtCo/C	0.1	0.1	1.01	603	0.2	
PtRhCu@Pt/C	0.2	0.2	0.6#	529	0.15	**10**
Pt_3FeCo NSs/C	0.30	0.18	1.45	900#	without	**11**

References

1 J. Lim, H. Shin, M. Kim, H. Lee, K.-S. Lee, Y. Kwon, D. Song, S. Oh, H. Kim and E. Cho, *Nano Letters*, 2018, **18**, 2450-2458.

2 X. Tian, X. Zhao, Y.-Q. Su, L. Wang, H. Wang, D. Dang, B. Chi, H. Liu, E. J. M. Hensen, X. W. Lou and B. Y. Xia, *Science*, 2019, **366**, 850-856.

3 J. Liang, Z. Zhao, N. Li, X. Wang, S. Li, X. Liu, T. Wang, G. Lu, D. Wang, B.-J. Hwang, Y. Huang, D. Su and Q. Li, *Advanced Energy Materials*, 2020, **10**, 2000179.

4 Y. Liu, C. Zhan, J. Zhang, X. Huang and L. Bu, *Journal of Materials Chemistry A*, 2023, **11**, 1455-1460.

5 W. Zhu, Y. Pei, H. Liu, R. Yue, S. Ling, J. Zhang, X. Liu, Y. Yin and M. D. Guiver, *Advanced Science*, 2023, **10**, 2206062.

6 J.-H. Park, N. Saito and M. Kawasumi, *Carbon*, 2023, **214**, 118364.

7 L. Sun, Y. Yin, B. Ren, Y. Qin, G. Wen and Z. Chen, *Nano Energy*, 2024, **120**, 109154.

8 C. Gyan-Barimah, J. S. P. Mantha, H.-Y. Lee, Y. Wei, C.-H. Shin, M. I. Maulana, J. Kim, G. Henkelman and J.-S. Yu, *Nature Communications*, 2024, **15**, 7034.

9 Y. Deng, L. Zhang, J. Zheng, D. Dang, J. Zhang, X. Gu, X. Yang, W. Tan, L. Wang, L. Zeng, C. Chen, T. Wang and Z. Cui, *Small*, 2024, **20**, 2400381.

10 Z. An, H. Li, X. Zhang, Z. Xia, H. Zhang, W. Chu, S. Yu, S. Wang and G. Sun, *ACS Catalysis*, 2024, **14**, 2572-2581.

11 L. Bu, J. Liang, F. Ning, J. Huang, B. Huang, M. Sun, C. Zhan, Y. Ma, X. Zhou, Q. Li and X. Huang, *Advanced Materials*, 2023, **35**, 2208672.